Determining Forming Limit Diagrams of Annealed 304 Stainless Steel at Multiple Strain Rates Using Digital Image Correlation

By: Elliott Harrod
Department of Mechanical and Aeronautical Engineering
Dynamic Mechanics of Materials Laboratory
Advisor: Dr. Amos Gilat

ABSTRACT

Forming Limit Diagrams are an essential tool in the metal forming industry. They accurately estimate the overall deformation a material can endure without ripping or wrinkling. Obtaining and modeling these curves can be a difficult process, especially with rate-sensitive material. Rate-sensitive material may affect the Forming Limit Diagram and limit the speed at which metal forming can occur. Nakajima Testing is a prominent method of obtaining a Forming Limit Diagram, as per ISO 120004-2.

This paper aims to examine the behavioral changes of the Forming Limit Diagram of annealed 304 Stainless Steel at two different strain rates, quasi-static and dynamic. Quasi-static tension testing is performed and localized strain data is used in LS-DYNA to simulate future Nakajima Testing. Nakajima Testing is performed using a fixture that is used on a hydraulic load frame at a quasi-static rate, and on a drop tower apparatus at a dynamic rate. The quasi-static test results and dynamic test results are compared with each other, as well as the simulated results. The dynamic testing resulted in a higher FLD than the quasi-static testing. More testing needs to be performed to solidify the results.

INTRODUCTION

Forming Limit Diagrams (FLD) are a necessary tool used in manufacturing processes daily. They provide manufacturers with information regarding how much material deformation can occur without wrinkling or tearing. This directly determines the blank geometry and number of forming processes in stamping, forming and drawing. [1]

An FLD is a graphical representation of material deformation until failure. The graph includes a line of different specimen geometries' principal strains. The major strain is plotted on the Y-axis and the minor strain is plotted on the X-axis. As long as manufacturers are induced strain is under this line, the part that is being stamped will not fail. In other words, an FLD is a guideline for direct response of sheet metal under forming conditions.

There are two ways of determining an FLD. The first is through simulation. The Marciniak and Kuczynski Method, or M-K Method simulates an FLD through use of FEM. This allows for the predictive behavior of the material and is compared with experimental data. The M-K Method can be used for many material models. Due to the method of calculation, the M-K Method cannot be used for rate sensitive material. The method only allows for one stress strain input. [2] The second method uses experimental data. This is known as the Nakajima Method. The Nakajima Method is an ISO standard that is widely used in industry. The test includes punching a round specimen and then repeating the tests while removing small amounts of material in the specimen geometry. [3] This method validates the M-K Method. The downsides of using the Nakajima Method is that the FLD is only valid for the material that is tested. The method does incorporate rate sensitivity into the results.

EXPERIMENT PREPARATION

Tension Testing:

Uniaxial tensile testing was performed to gather experimental data for the LS-DYNA simulation of the Nakajima Testing. The specimens were made according to the ASTM E3 standard and cut with a water-jet machine. The testing was performed on a 200kN MTS 370.25 Landmark hydraulic load frame. The tests were performed at a quasi-static strain rate of $1e^{-3}/s^{-1}$. Strain measurement of the testing was performed by using a 3D digital image correlation system, VIC-3D. Two Grey Point Gazelle cameras were placed equidistant from the specimen equipped with 35mm lenses. Prior to testing, the specimen was coated with white paint and a black paint speckled pattern. This black speckle pattern was made by spraying spray paint from a distance. The image acquisition system, VIC-Snap, was started before the MTS program began operating. VIC-Snap recorded an image of the specimen at a rate of 2 frames per second. Each time an image is taken, the system would also record time, actuator position, and load. After specimen failure, the images were correlated with VIC-3D. The software parameters used a subset of 21, a step size of 2, and a filter of 5. The strain was calculated in a hencky tensor. The strain in the vertical direction at the point of failure was extracted and further analyzed.

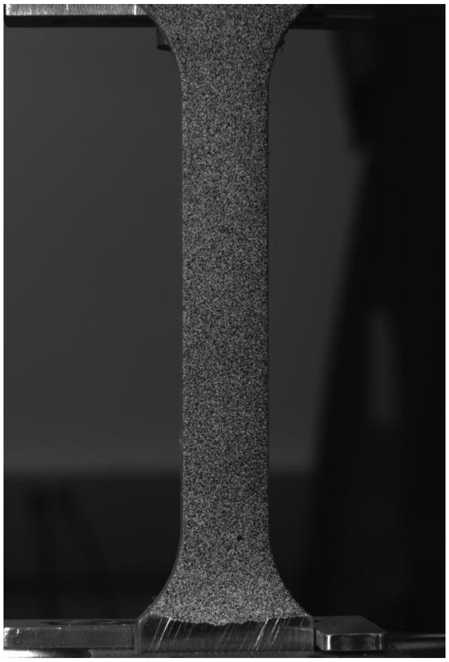

Figure 1: ASTM E8 Tension Test with Speckle Pattern

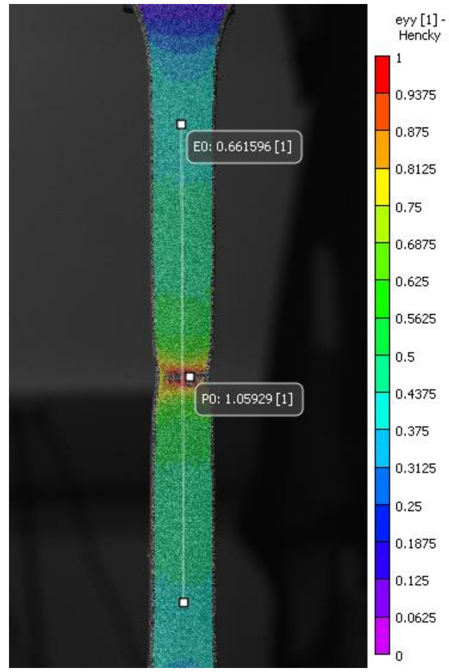

Figure 2: VIC-3D Strain Calculation

The true stress and true strain at the point of failure of each specimen was calculated with the data extracted from VIC-3D. This was done using the following calculations.

$$\sigma_{eng} = \frac{F}{A} \tag{1}$$

$$\varepsilon_{true} = \log(1 + \varepsilon_{eng}) \tag{2}$$

$$\sigma_{true} = \sigma_{eng}(1 + \varepsilon_{eng}) \tag{3}$$

A total of 3 tests were performed, and the test that performed the average of the three was selected for input to LS-DYNA.

Uniaxial Tensile Testing					
Test #	Gage Length (mm)	Thickness (mm)	Width (mm)	Strain at Failure	Stress at Failure (MPa)
1	57.15	12.63015	2.56667	1.09595	1618.062157
2	57.15	12.6238	2.56921	1.05929	1609.056066
3	57.15	12.6238	2.57048	1.05571	1580.728284

Table 1: Uniaxial Tensile Test Results

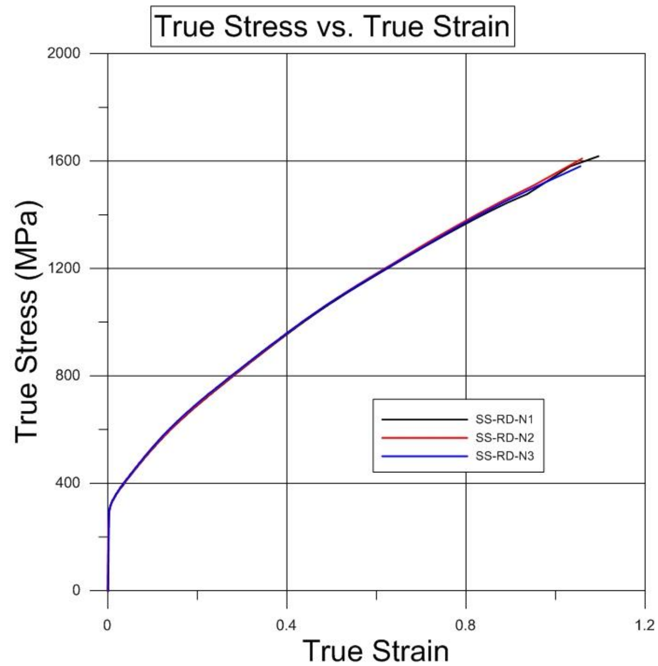

Figure 3: Stress-Strain Curve of Tension Testing

All three tests were consistent, and the second test was chosen for input into LS-DYNA.

Simulation:

The plastic region of the curve was extracted and imported into the Livermore Software Dynamic solver. The input deck used for the simulation used in the simulation depended on kinetic energy and hourglassing. The simulation had a termination time of 20 milliseconds. The model consisted of two rigid clamps on the upper and lower section of the specimen with a tied surface to surface contact method. The punch was a 43.18 mm steel punch. The punch was given an initial velocity of 4000 mm/s to pierce the specimen. The specimen material was given the linear piecewise plasticity model, which was determined from the tension testing above.

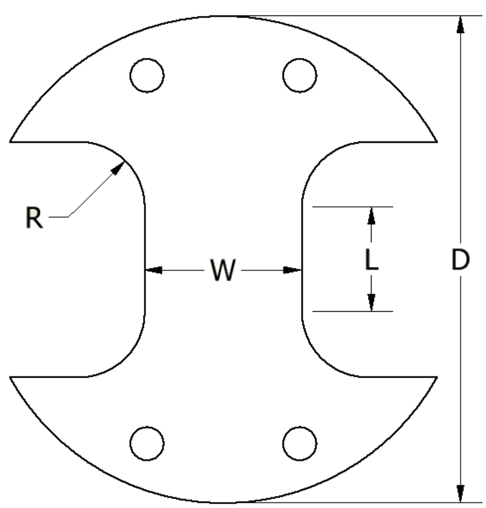

Figure 4: Specimen Geometry for Simulation

The specimen geometry had a given value for R = 18.17 mm, L = 30 mm, and D = 139.7 mm. The gage width, W, was simulated with 7.5 mm, 15 mm, 45 mm, 60 mm, 80 mm and 139.7mm. The clamp geometry consisted of a flat ring with an ID = 76.2 mm and OD = 139.7 mm. All components were made in Inventor and meshed using HyperMesh. Several simulations were run to determine the specimens would not rip along the 76.2 mm opening in the clamps. An analysis of the principle strains from the simulation helped in determination of specimen geometry as well.

Four specimen geometries were determined for appropriate for testing their varying gage width is shown below:

Geometry	Width (mm)	Expected State
A	15	Tension
B	45	Mixed
C	65	Mixed
D	139.7	Biaxial

Table 2: Gage Width Parameters with Expected Strain State

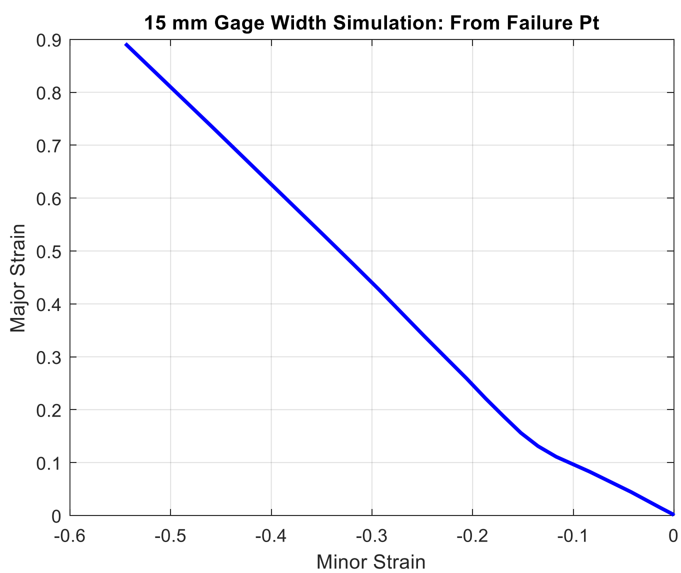

Figure 5: Simulation of 15mm Specimen

The 15 mm simulation showed interesting results which are promising for testing. In the figure above, the principle stains are graphed. The path toward failure of the specimen is linear in direction and close to pure uniaxial tension. Similar results are expected below.

EXPERIMENTS

Fixture:

The test fixture used was designed to allow images to be taken of the specimen without risk of damage to the cameras. The fixture consists of four columns supporting a 76.2 mm in diameter die. A clamp is applied to the top of the die and a mirror is placed in between the four pillars at a 45-degree angle.

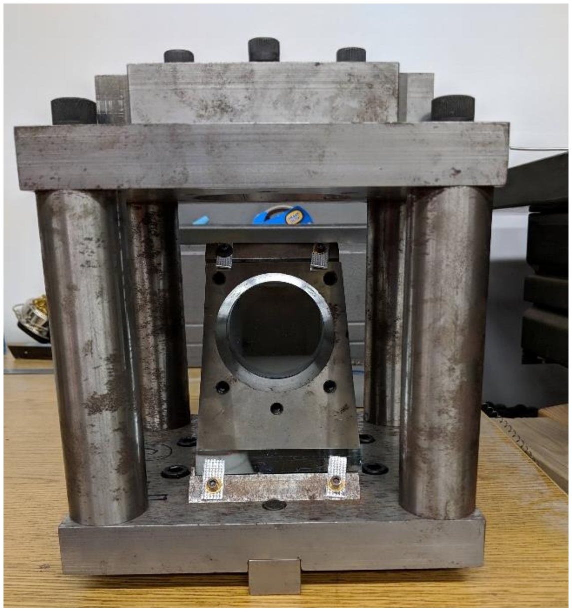

Figure 6: Front View of Fixture

Figure 7: Side View of Fixture

Quasi-static Testing:

The fixture was placed on the 200kN MTS 370.25 Landmark hydraulic load frame with a DIC setup of 2 gazelle cameras equipped with 35 mm lenses. The DIC system was calibrated using a 4 mm calibration panel. The DIC acquisition system was set up to record an image at two frames per second. Each time an image is recorded, time, stroke, and load data are also recorded. The load frame was programmed to move the 25.4 mm punch at a rate of 76.2 mm / 900 s.

Figure 8: Image of 15 mm Specimen on Hydraulic Load Frame

A total of six tests were performed; Two 139.7 mm, one 65 mm, one 45 mm, one 15 mm with a 25.4 mm punch and one 15 mm with a 43.18 mm punch.

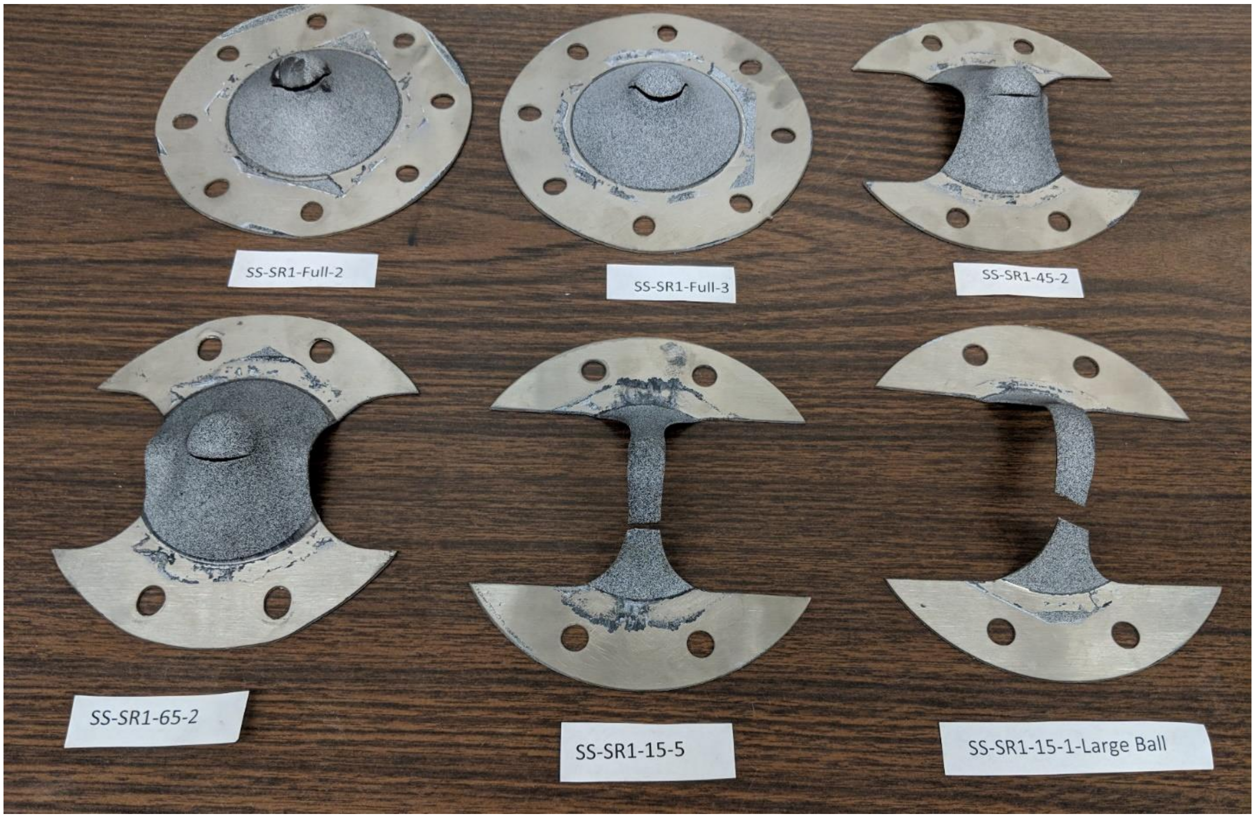

Figure 10: Picture of Quasi-static specimens after failure

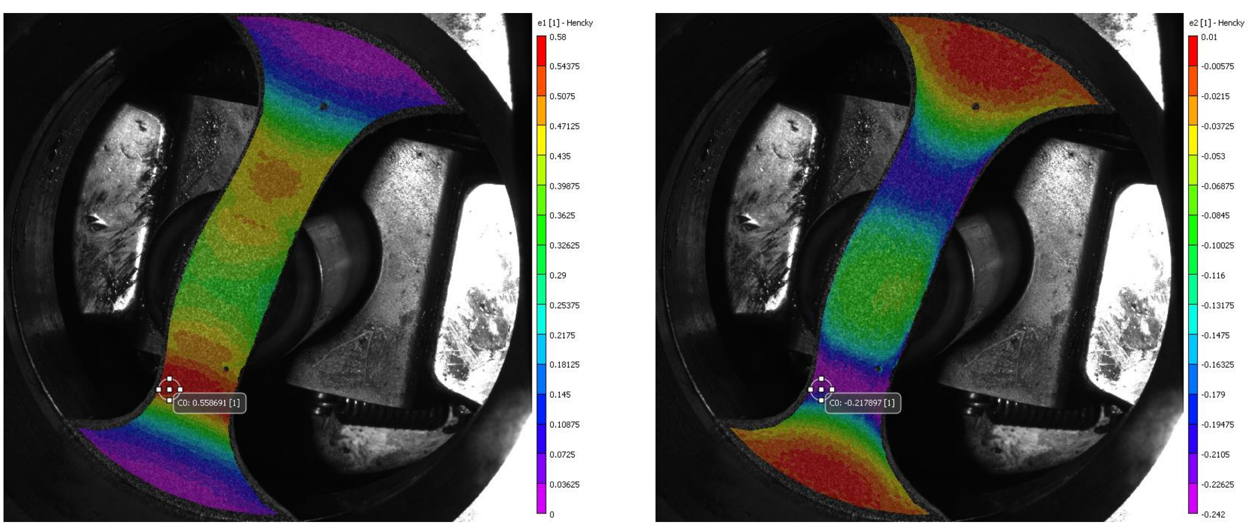

Figure 9: Digital Image Correlation of 15 mm Specimen

Digital Image Correlation of each specimen was performed and their principal strains were extracted from the point of failure. The parameters used for DIC were a subset of 21, a step size of 2, and a filter of 5.

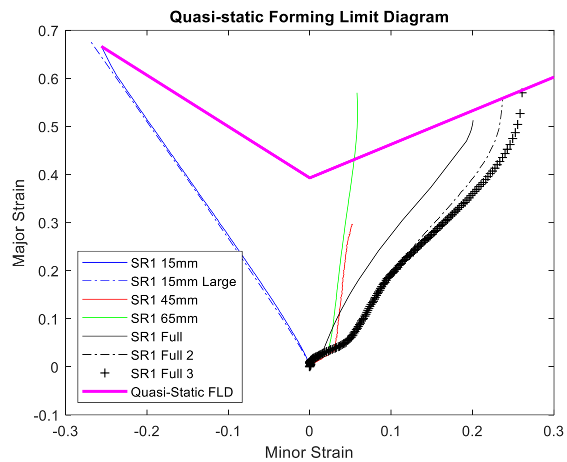

Figure 11: Principal Strains for Quasi-Static Testing

The principle strains of each test were plotted and analyzed to make a FLD. The 15 mm strains showed near uniaxial tension, but the other tests were not clear. The 45 mm and 65 mm specimens showed close to plane strain failure, but the 65 mm specimen had much higher strain in the major direction. The full specimen tests were not pure biaxial strain, but were included in the FLD calculation.

Dynamic Testing:

Dynamic testing was performed using a Dynatup 8120 drop tower apparatus. The Dynatup was loaded with 226.796 kg of lead weight and dropped with an impact speed of 4.2 m/s. The drop tower was equipped with a 135 kN load cell that was calibrated prior to the experiment. The same fixture used in the quasi-static testing was used in this experiment. The positioning of the 25.4 mm punch was determined set in alignment of the center of the die using a laser. The DIC acquisition system consisted of two Photron SA1.1 cameras equipped with 100 mm lenses. The system was operated through fastcam at an acquisition rate of 20,000 frames per second. The system was triggered with a manual switch at the time the weight was released.

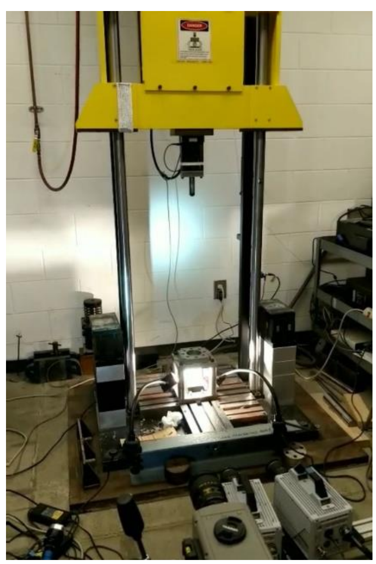

Figure 12: Drop Tower Apparatus

A total of four tests were performed; one 139.7 mm, one 65 mm, one 45 mm, one 15 mm.

Figure 13: Picture of Dynamic Specimens After Failure

Digital Image Correlation of each specimen was performed and their principal strains were extracted from the point of failure. The parameters used for DIC were a subset of 21, a step size of 2, and a filter of 5.

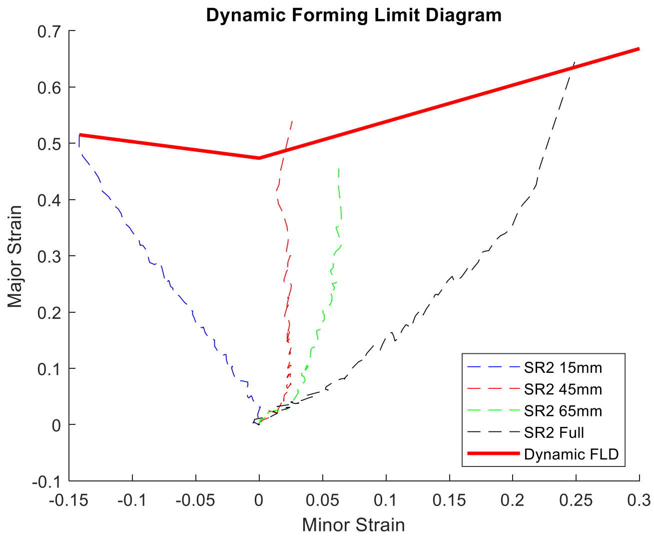

Figure 14: Principal Strains for Dynamic Testing

The principle strains of each test were plotted and analyzed to make a FLD. The 15 mm strains showed near uniaxial tension, but had much lower strain in the minor direction. The 45 mm and 65 mm specimens showed close to plane strain failure, but the 45 mm specimen had slightly higher strain in the major direction. The full specimen tests were not pure biaxial strain, but were included in the FLD calculation.

Conclusion:

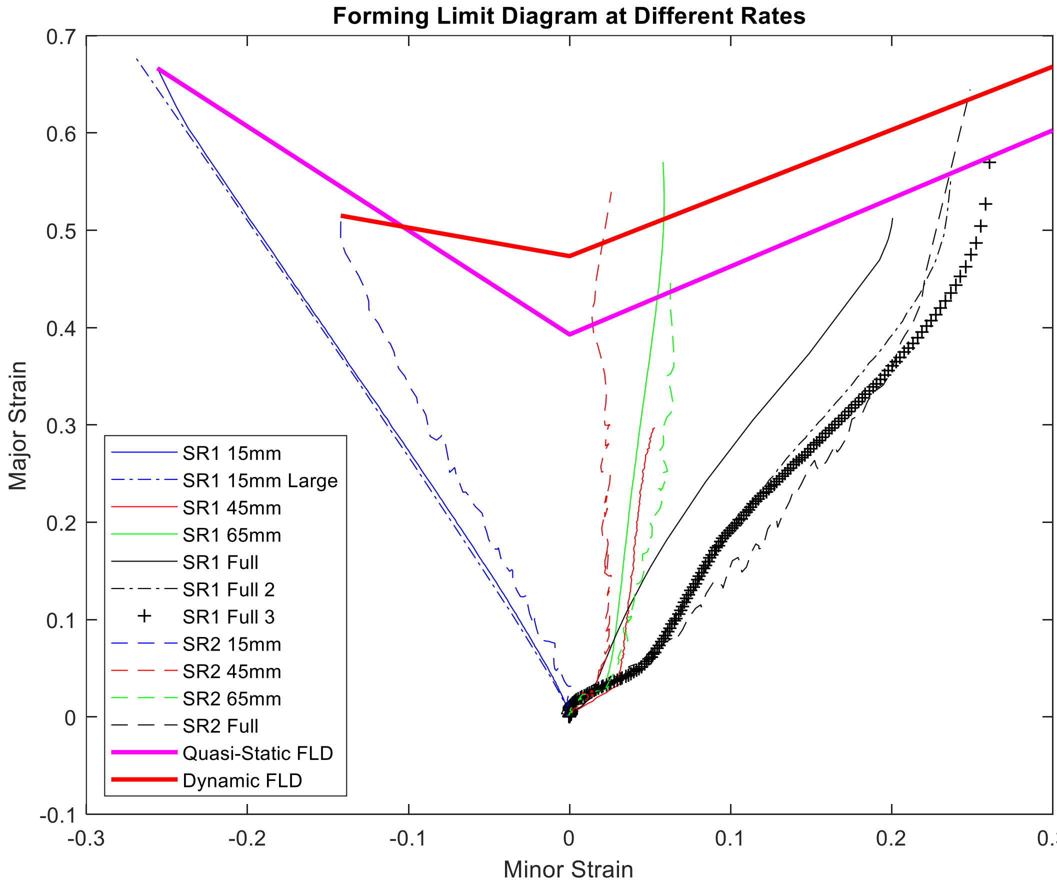

Figure 15: Plot of Both Quasi-static and Dynamic Testing

Overlaying the Quasi-static FLD with the Dynamic FLD shows signs of strain rate sensitivity. The dynamic testing resulted in much higher strain in the major direction. This may be due to lack of thermal dissipation during the dynamic tests. Due to the outliers produced during the testing of the 45 mm and 65 mm specimen, the results are determined inconclusive. More testing needs to be performed to determine the actual FLD at both rates. This would include investigation of thermal properties at different rates, incorporating multiple punch sizes, and more specimen geometries.

References:

[1] Mohammed, Bassam & Park, Taejoon & Pourboghrat, Farhang & Hu, Jun & Esmaeilpour, Rasoul & Abu-Farha, Fadi. (2017). Multiscale Crystal Plasticity Modeling of Multiphase Advanced High Strength Steel. International Journal of Solids and Structures. 10.1016/j.ijsolstr.2017.05.007.

[2] B. L Ma, M. Wan, Z. Y Cai, W. N Yuan, C. Li, X. D Wu, W. Liu, Investigation on the forming limits of 5754-O aluminum alloy sheet with the numerical Marciniak–Kuczynski approach, International Journal of Mechanical Sciences, Volumes 142–143, 2018, Pages 420-431, ISSN 0020-7403

[3] Nathalie, Weiß-Borkowski & Lian, Junhe & Marten, Thorsten & Tröster, Thomas & Muenstermann, Sebastian & Bleck, Wolfgang. (2017). Forming limit curves determined in high-speed Nakajima tests and predicted by a strain rate sensitive model. AIP Conference Proceedings. 1896. 020004. 10.1063/1.5007961.